MODELING AND SIMULATION OF A MICROSYSTEM WITH SPICE SIMULATOR

I. Zelinka, J. Diaci*, V. Kunc, L. Trontelj,
Faculty of Electrical Engineering, University of Ljubljana, Slovenia
*Faculty of Mechanical Engineering, University of Ljubljana, Slovenia

Keywords: MST, MicroSysTems, definitions, simulations, nondifferential capacitive measurements, bipolar measuring ranges, capacitive micromechanical sensors, CAST, Custom Application Specific Technology, development trends, mechanical analysis, SPICE model, actuating capacitors, measuring capacitors

Abstract: In the paper Microsystem (MST) definition and development trends are described. Modeling of a capacitive micromehanical sensor is presented. Verification of dynamical behavior is analized. Mechanical analysis and the SPICE model of the mechanical part of the sensor are shown.

Modeliranje in simuliranje mikrosistema s simulatorjem SPICE

Ključne besede: MST mikrosistemi, definicije, simulacije, meritve kapacitivne nediferencialne, območja merilna dvosmerna, senzorji mikromehanski kapacitivni, CAST tehnologija specifična uporabniško aplikacijska, smeri razvoja, analiza mehanska, SPICE model, kondenzatorji aktivatorski, kondenzatorji merilni

Povzetek: Opisana je definicija mikrosistema (MST) in razvojni trendi. Prikazano je modeliranje kapacitivnega mikromehanskega senzorja in analizirano je dinamično obnašanje sistema. Podana je mehanska analiza in SPICE model mehankega dela senzorja.

1 INTRODUCTION

The basic difference between ICs and microsystems is shown on Fig. 1. While ICs mostly handle information, MSTs usually deal with energy. They always represent the complete system required to perform the desired function.

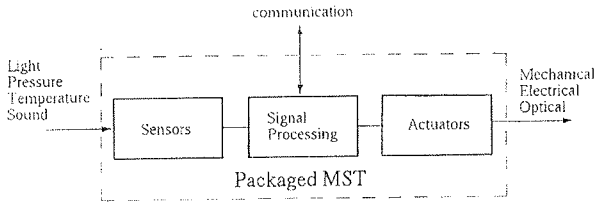

Fig. 1: Microsystem definition

The introduction of microsystems followed the same basic rules which promoted the development of ICs. They are small and require low power. A large number of them can be manufactured simultaneously, thus offering lower costs and greater reproducibility. In addition, the ratio of performance versus price is far superior to that of the lumped versions.

Two basic differences in comparing ICs and MSTs are essential: only few atoms are required to handle information in a well optimized and carefully designed IC, while the dimension of MST depends on the amount of energy to be manipulated. Therefore the same scaling rules as well as Moore's Law do not apply.

Development trends of ICs are still widely governed by the development of optical lithography. We see the advent of 0.18 μm custom application specific technology (CAST) for volume production and a substantial increase of the diameter of silicon wafers. Tools for the development of photoplates capable to be used together with the advanced imaging techniques are emerging.

On the contrary, the smaller and finer geometries in MSTs are not vital or even possible considering the amount of energy to be handled in specific application. Therefore the MST related activities are reserved for those environments of design and production which are not able to compete in the every day financially more demanding new equipment procurement and refined fab environment associated with the deep submicron technologies. Therefore, it is viable that the Laboratory for Microelectronics (LMFE) aggressively entered the new exciting field of MSTs, offering new applications in the fields of data storage, displays, communications, IR imaging, biochips, micromachines, and microinstruments.

Although there exist remarkable simulation tools, which offer great support to a designer confronted with specific design problems in the field of electrical/electronic or mechanical engineering, there's a very acute lack of simulation software which would allow efficient solutions to coupled electromechanical problems, which are commonly encountered in the field of MSTs. The gap between the two engineering disciplines seems to be too large in any practical situation requiring a solution of coupled electromechanical problems to allow a

microsystems designer to benefit from a coherent use of existing mechanical and electronic design packages.

Different schemes exist to construct a micromechanical part of the sensor. However, one which uses a cantilever seems to be the most promising, offering the largest sensitivity for a given size /2/. In the paper we present a non differential capacitive MST sensor which also has definite production advantages over the two capacitor version, but it requires more effort to model it properly. We have adapted the equations describing the micromechanical part of the sensor in a form acceptable as an input to the standard electronic analog simulator. This gives us the ability of prediction of a closed loop behavior of both parts of the system.

In the paper we present the analysis and modeling for the chosen MST.

The elastic element of the sensor acts as one plate of the sensing and actuating capacitor. Deformation of the elastic element, due to external loads (related to the measured physical quantities), are counteracted by the electronic servosystem, which consists of a capacitive sensor, actuator and signal processing electronics. In the dynamic equilibrium, the actuating electrical force equals the external load. From the parameters influencing the actuating force the external load and the related physical quantities can be determined.

2 STATIC ANALYSIS

The configuration of a single capacitor model is on Fig. 2.

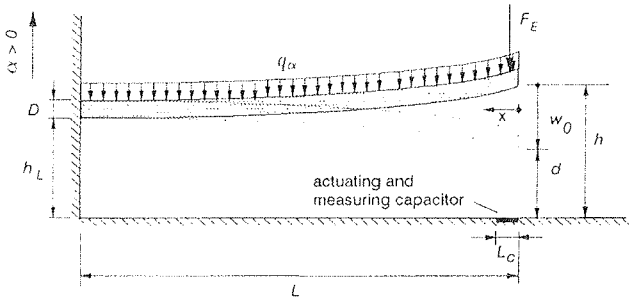

Fig. 2: Cantilever with one capacitor for actuating and measuring

The basic equation for deflection w of the cantilever loaded with distributed load q is /3, 4/:

$$EI\frac{d^4w}{dx^4} = q \qquad (1)$$

where E is Young's modulus, I is the area moment of inertia, w=w(x) and x is measured from the tip towards the clamped end of the beam. The boundary conditions are: at clamped end: w(L)=0
w'(L)=0
at free end: w''(0)=0
w'''(0)=0
For the special case of point force F load we take q = Fδ(0). The deflection of the beam depends on loads. We consider the beam (cantilever) loaded with one distributed external load q_α, and point electrostatic force F_E. We can assume electrostatic force as a point force if capacitor length (L_c) is less than 10% of beam length (L) /5/.

For distributed load w_q or point force w_F we have the following equations describing the deflection /3/:

$$w_q(x) = \frac{qL^4}{24EI}\left[3 - 4\left(\frac{x}{L}\right) + \left(\frac{x}{L}\right)^4\right] \qquad (2)$$

$$w_F(x) = \frac{FL^3}{6EI}\left[2 - 3\left(\frac{x}{L}\right) + \left(\frac{x}{L}\right)^3\right] \qquad (3)$$

Of special importance for the analysis are the deflections of the beam tip:

$$w_q(0) = \frac{qL^4}{8EI} \qquad (4)$$

$$w_F(0) = \frac{FL^3}{3EI} \qquad (5)$$

According to the principle of superposition, the total deflection w(x) under combined loads is the sum of the two contributions:

$$w(x) = w_q(x) + w_F(x) \qquad (6)$$

In order to examine the stability of the system, we assume the beam loaded with one distributed load q_α and point electrostatic force F_E. With introducing new variables $k_F=3EI/L^3$ and $k_q=8EI/L^3$, which represent stiffness of the beam, we can write eq.(6) for the deflection of the beam tip

$$w_0 = w_F + w_q = \frac{F_E}{k_F} + \frac{q_\alpha L}{k_q} \qquad (7)$$

In general, F_E is a sum of the electrostatic forces of actuation and measuring. Therefore this equation is valid for an open loop system (no actuation voltage, electrostatic force only due to read-out voltage) and for a closed loop (voltage driven) with one or two capacitors. We seek solutions from the above equation for w_0 subject to the obvious restriction $w_0 < h$.

By inserting

$$F_E = F_e\frac{h^2}{(h - w_0)^2} \qquad (8)$$

where $F_e=1/2\ \varepsilon\ A\ (U/h)^2$ in eq.(7) and by introducing dimensionless variables

$$W_0 = \frac{w_0}{h}; \qquad K = \frac{F_e}{k_F h}; \qquad W_\alpha = \frac{m\alpha}{k_q h}$$

we can write eq.(7) in form

$$W_0 = K\frac{1}{(1-W_0)^2} + W_\alpha \qquad (9)$$

To find the solution, we rewrite the above equation in the form of a cubic:

$$W_0^3 - (W_\alpha + 2)W_0^2 + (1+2W_\alpha)W_0 = K + W_\alpha \qquad (10)$$

With finding the maximum of the l.h.s. of expression (10) we get the stability limits:

$$W_0 < \frac{1+2W_\alpha}{3} \quad \Leftrightarrow \quad K < \frac{4}{27}(1-W_\alpha)^3 \qquad (11)$$

The system is stable when either of the above inequalities hold. With the additional condition K>0 we get a range of possible solutions:

$$W_\alpha < W_0 < \frac{1+2W_\alpha}{3} \quad \Leftrightarrow \quad W_0 < W_\alpha < \frac{3W_0 - 1}{2} \qquad (12)$$

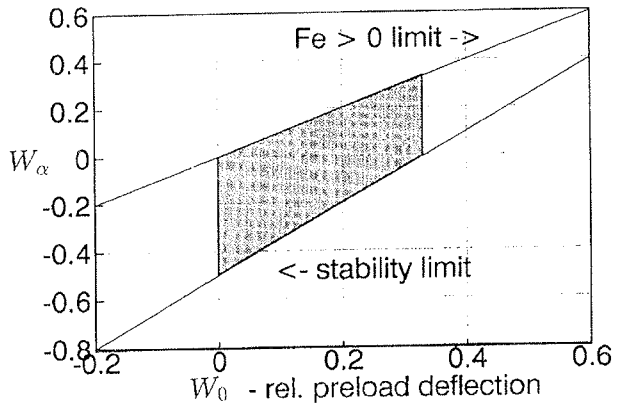

Fig. 3: Rel. measured load (W_α) vs. rel. preloading (W_0) - shaded area shows the useful range for bipolar measurement

POSITIONING OF THE BEAM

Since the electrostatic force can not change polarity, we have to preload the beam with a static actuating force F_{E0} and move the beam tip by w_0 below its initial distance h if we want to measure load in both directions. The stability diagram on Fig.(3) shows that in principle we can perform bipolar measurement for any relative preloading in the range $0<W_0<1/3$. To accommodate the required range $\alpha_{min}<\alpha<\alpha_{max}$ at a selected W_0 we have to select the appropriate beam stiffness (via thickness change). We can select W_0 according to different criteria. We will take a closer look at just one - Maximization of dynamic range.

There is exactly one value $W_{0\delta}$ where we can fit the required load range $\alpha_{min}<\alpha<\alpha_{max}$ without any waste of the dynamic range. To calculate $W_{0\delta}$, we equate the lower and the higher bound value for W_0 in eq.(12) and insert the ratio: $r_\alpha=\alpha_{min}/\alpha_{max}=W_\alpha/W_\alpha$. The result is:

$$W_{0\delta} = 1/(3-2r_\alpha) \qquad (13)$$

Example: for the symmetrical bipolar range we have r_α=-1 and $W_{0\delta}$=1/5.

If we select our W_0 above $W_{0\delta}$, then the corresponding W_α value is smaller than optimal and we have to increase the beam stiffness/mass ratio k_q/m (increase thickness D) to be able to measure the required α_{min}. We will waste some dynamic range on the positive side then, because the corresponding mass, stiffness and $W_\alpha$max would allow the measurement of higher max. load than required by α_{max}. The opposite happens when we select W_0 below the optimal value. We have to design beam thickness according to α_{max} and thus waste some dynamic range below α_{min}. We can summarize this discussion with the following formulae:

$$W_0 > W_{0\delta}: W_{\alpha min} = (3W_0 - 1)/2 \Rightarrow D = \sqrt{\frac{3\rho L^4 \alpha_{min}}{Eh(3W_0 - 1)}} \qquad (14)$$

$$W_0 < W_{0\delta}: W_{\alpha max} = W_0 \quad \Rightarrow D = \sqrt{\frac{3\rho L^4 \alpha_{max}}{2EhW_0}} \qquad (15)$$

There are, of course, practical limitations to D; therefore we shouldn't expect to be able to realize the beam when the selected W_0 is close to 1/3 or 0.

3 DYNAMIC ANALYSIS

In general, we can have a system with two capacitors that are not located on the same plane. For the analysis of dynamic behavior, we use the system configuration shown on Fig.(4).

The capacitor sizes estimated by using the point capacitor models show that in practice both capacitors (meas-

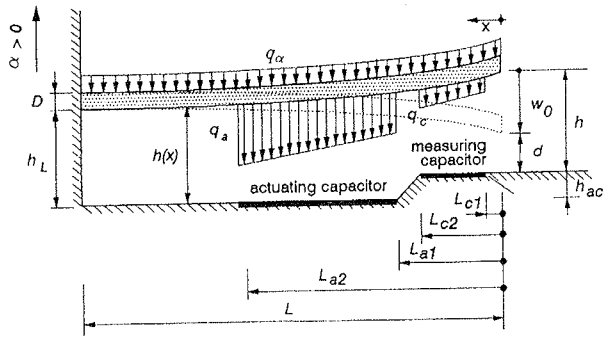

Fig. 4:Cantilever with two distributed capacitors

uring and actuating) should have lengths larger than 10% of the length of the beam. For this size, the inter-plate spacing variations within each capacitor are not negligible and we have to treat the capacitors as distributed along the beam. We model the electrostatic forces as distributed loads:

$$q_i(w,x,t) = \frac{1}{2}\varepsilon_i B U_{ri}^2 \frac{\Pi(x,L_{i1},L_{i2})}{[h(x)-w(x)]^2}$$

$$\text{with:}\quad \Pi(x,L_{i1},L_{i2}) = \begin{cases} 1 & \text{for: } L_{i1} \le x \le L_{i2} \\ 0 & \text{elsewhere} \end{cases} \qquad (16)$$

where i=a for the actuating and i=c for the measuring capacitor. B and U_{ri} represent the width of the beam and applied voltage respectively. For the analysis of dynamic behavior dumping and moment of inertia have to be considered also. Inserting the two loads into the basic eq.(1) we describe the deflection w(x,t) of the beam by the following boundary problem:

$$\rho DB\ddot{w}(x,t) + q_d(\dot{w},w,x,t) + EI\frac{\partial^4 w(x,t)}{\partial x^4} =$$

$$= q_a(w,x,t) + q_c(w,x,t) + q_\alpha(t) \qquad (17)$$

$$w(L,t) = 0$$

$$w'(L,t) = 0$$

$$w''(0,t) = 0$$

$$w'''(0,t) = 0$$

where $\rho DB\,\ddot{w}(x,t)$ represents the moment of inertia and $q_d(\dot{w},w,x,t)$ dumping. q_a and q_c are substituted with eq.(16) and $m\alpha(t)/L = \rho DB\alpha(t)$.

Electrical inputs to the mechanical part (from the electronic part of sensor) are voltages on actuating capacitor ($U_a(t)$) and measuring capacitor ($U_c(t)$). The output for the electronic part is measuring capacitance C(t) of the air gap capacitor:

$$C(t) = \varepsilon_c B \int_{L_{c1}}^{L_{c2}} \frac{dx}{h(x)-w(x,t)} \qquad (18)$$

For solving the upper equation we need function h(x), describing the initial form of the beam. Assuming a uniform distribution of the residual stress along the beam results in a parabolic form and the height function is defined as:

$$h(x) = h_L + (h_0 - h_L)(1 - x/L)^2 - h_{\alpha c}\Pi(x,L_{c1},L_{c2}) \qquad (19)$$

where h_0 and h_L are the initial heights of the tip and the clamped end respectively, measured relative to the base line, defined by the actuator plate, and where $h_{\alpha c}$ is the elevation of the measuring capacitor plate above the actuator plate.

The damping force $q_d(\dot{w},w,x,t)$ is strictly speaking the solution of a special squeezed-film air-flow boundary problem. We find that it would be quite impractical to try to solve it by means of electrical analogies using an electronic simulation codes, such as SPICE. Instead of that, we suggest the use of an approximate analytical solution of the varying gap squeezed-film boundary problem /6, 7/:

$$q_d(\dot{w},w,x,t) = b(w,x)\dot{w}(x,t) \qquad (20)$$

where

$$b(w,x) = 12\mu BL^2 \frac{\left(1 - \dfrac{\cosh\left(\sqrt{12(L-x)/B}\right)}{\cosh\left(\sqrt{12L/B}\right)}\right)}{[h(x)-w(x,t)]^3} \qquad (21)$$

4 MODELING

Usually approaches to modeling /8, 9, 10/ are based on substituting mechanical elements with equivalent electrical elements (Fig. 5).

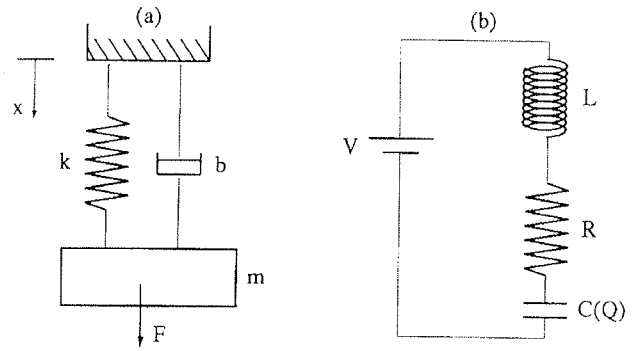

Fig. 5: Mechanical system and (b) equivalent electrical circuit

The equation describing a single mass mechanical system

$$m\ddot{x} + b\dot{x} + kx = F_a + F_c + q \qquad (22)$$

is similar to the equation describing electrical circuit on Fig. (5b)

$$L\frac{di}{dt} + Ri + \frac{1}{C}\int i\,dt = V \qquad (23)$$

where

$$\dot{x} \equiv i \quad x \equiv \int i\,dt \quad m \equiv L \quad b \equiv R \quad k \equiv \tfrac{1}{C}$$

The equation describing the behavior of the cantilever beam (eq. 17) can be substituted with eq.(22) only when the mechanical system with the single degree of freedom is assumed. Modeling (substitution) of our cantilever beam with single mass mechanical system on Fig.(5a) does not give satisfactory accuracy.

Our modeling of differential equation follows the work of Herbert /11/ and Pelz /12, 13/. All state variables in the equation, e.g. velocity, deflection are represented by node voltages.

Nonlinear dependent voltage controlled voltage sources are used to determine the state variables of the highest time derivatives and the algebraic equations. Simple integrators calculate the values for the lower derivatives.

For example, the equation for distributed load q_α (load due to electrostatic force of actuating capacitor) from eq.(16) can be written in HSPICE by using Behavioral voltage source in form:

```
E_q_a q_a 0 vol='((0.5*eps*B*(v(Urefa)**2))/
/((v(hx)-v(w))**2))'
```

where eps and B are defined as parameters. In this way, systems of algebraic and ordinary differential equations can be solved.

The output from the mechanical part and the input for the electronic part is capacitance of the measuring capacitor:

$$C(t) = \varepsilon_c B \int_{L_{c1}}^{L_{c2}} \frac{dx}{h(x) - w(x,t)} \qquad (24)$$

In order to solve the upper equation, the initial form (height) of cantilever h(x) has to be known and the deflection w(x,t) calculated. For h(x) we take eq.(19) where $h_{\alpha c}=0$

$$h(x) = h_L + (h_0 - h_L)(1 - x/L)^2 \qquad (25)$$

To get the w(x,t) we have to solve the boundary problem in the eq. (17), which we rewrite in order to get the highest time derivative on the l.h.s.

$$\ddot{w}(x,t) = -\frac{EI}{\rho DB}\frac{\partial^4 w(x,t)}{\partial x^4} - \frac{1}{\rho DB} q_d(\dot{w}, w, x, t)$$

$$+\frac{1}{\rho DB} q_\alpha(w, x, t) + \frac{1}{\rho DB} q_c(w, x, t) + \alpha(t) \qquad (26)$$

The proposed method of modeling does not allow direct modeling of partial differential equations or integration over spatial variable. With the implementation of some mathematical approximations, we can extend this work and solve the system of equations describing our cantilever beam. With the method of finite differences (FDM) /14, 15/, the spatial variables of partial differential equations are discretized and an algebraic equation is inserted for each node. Discretization schemes for spatial derivatives up to the fourth order /14, 15/ are:

$$\frac{\partial w(x,t)}{\partial x} \approx \frac{1}{12h} * \left(w_{x_{i-2}} - 8w_{x_{i-1}} + 8w_{x_{i+1}} - w_{x_{i+2}}\right) \qquad (27)$$

$$\frac{\partial^2 w(x,t)}{\partial x^2} \approx \frac{1}{12h} * \left(-w_{x_{i-2}} + 16w_{x_{i-1}} - 30x_i + 16w_{x_{i+1}} - w_{x_{i+2}}\right) \qquad (28)$$

$$\frac{\partial^3 w(x,t)}{\partial x^3} \approx \frac{1}{12h} * \left(-w_{x_{i-2}} + 2w_{x_{i-1}} - 2w_{x_{i+1}} + w_{x_{i+2}}\right) \qquad (29)$$

$$\frac{\partial^4 w(x,t)}{\partial x^4} \approx \frac{1}{12h} * \left(w_{x_{i-2}} - 4w_{x_{i-1}} + 6w_{x_i} - 4w_{x_{i+1}} + w_{x_{i+2}}\right) \qquad (30)$$

Each equation describes the behavior of the respective slot i, by regarding itself and some of its neighbours in both directions. In our case (eq. 26), w(x,t) is the function to be derived, and x is the spatial variable (for $0 \le x \le L$). The descretization step is h, and n is the number of discretization steps (h=L/n).

All equations containing the term $\partial^k w(x,t)/\partial x^k$, where k is the order of the derivative, have to be duplicated n times. The number of discretization steps n is the number of nodes. Eq. (26) for slot i is written in form for HSPICE using E source:

```
E_i w_i_tt 0 vol =

'(-konst1*(v(w_(i-2))-4*v(w_(i-1))+
+6*v(w_i)-4*v(w_(i+1))+v(w_(i+2)))

-konst2*v(q_d_i)+konst2*v(q_a_i)+
+konst2*v(q_c_i)+v(α))'
```

Values for konst1,konst2 are calculated and defined as parameters. Deflection w(x,t) is calculated with a simple integrator:

```
XINTEGRATOR_bi  w_i_tt  w_i_t INTEGRATOR

XINTEGRATOR_ai w_i_t  w_i INTEGRATOR
```

Index i represents respective slot ($0 \le i \le n$)

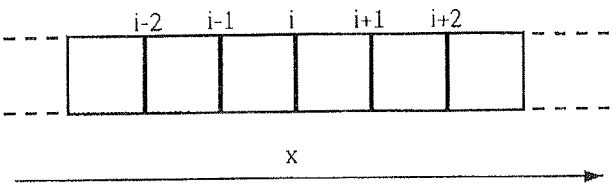

Fig. 6: Discretization of spatial variable x

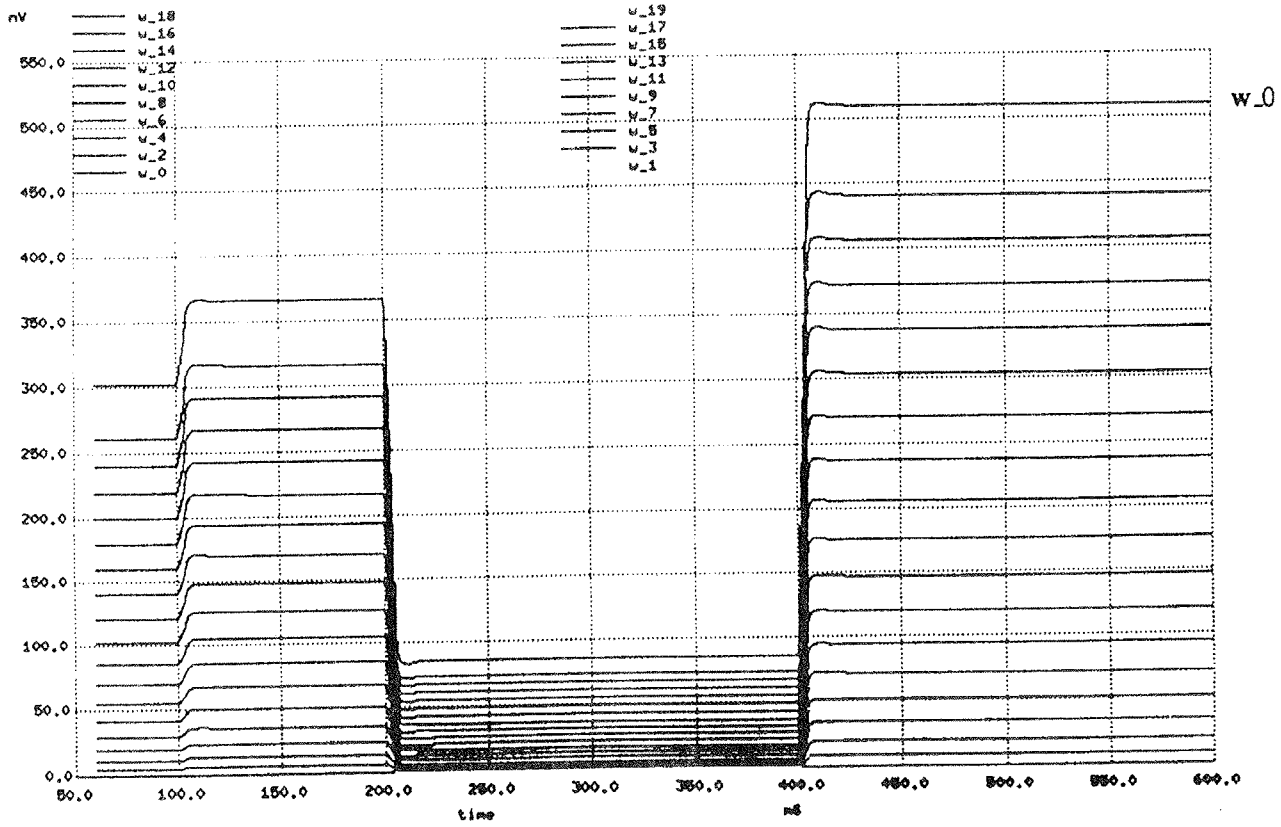

Fig. 7: Deflection of the beam for different discretization nodes

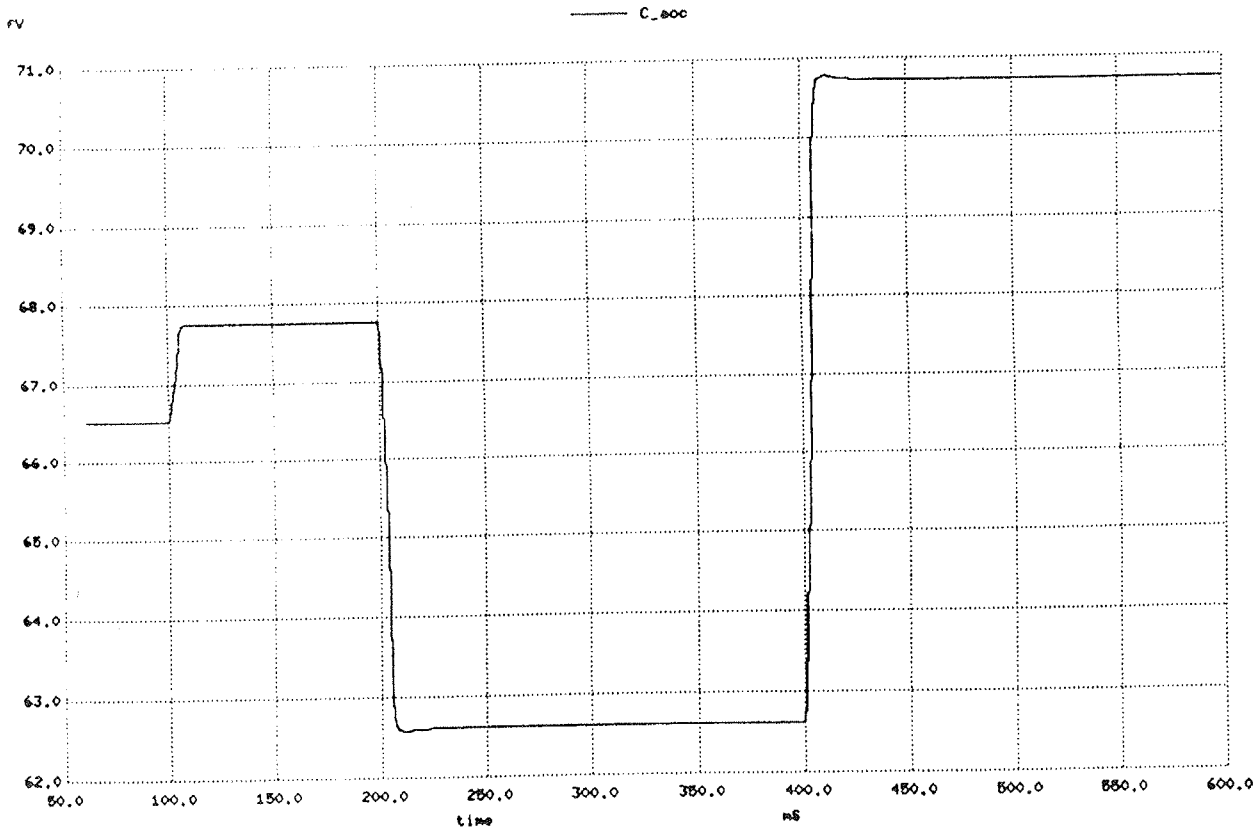

Fig. 8: Changing of measuring capacitance with changing of load

Spatial integrals are also discretized and substituted with algebraic equations following the Simpson's rule:

$$\int_a^b y dx \approx \frac{h}{3}(y_0 + 4y_1 + 2y_2 + 4y_3 + ... + 2y_{n-2} + 4y_{n-1} + y_n) \quad (31)$$

where h=(b-a)/n, with additional condition that n is an even number. So eq.(24) for capacitance of an air gap capacitor in form for HSPICE is as follows:

```
E_C_acc  C_acc  0 vol='epsilon*B*( 1/(v(hx_0) -
v(w_0)) + 4/(v(hx_1) - v(w_1)) + 2/(v(hx_2) - v(w_2)) +
4/(v(hx_3) - v(w_3)) + 1/(v(hx_4) - v(w_4)))'
```

The exact form of equation depends on the length of the measuring capacitor and the number of discretizations steps.

5 RESULTS

The results are shown on Fig. (7) and (8).

The calculation of the deflection for each node of discretized beam can be seen on Fig. (7) and the resulting capacitance of an air gap capacitor as an output of micromechanical part of sensor on fig. (8). The voltage representing capacitance can be transformed back to capacitance as input for the electronic part with use of Voltage controlled Capacitor.

6 CONCLUSIONS

The accuracy of a single mass model is not satisfactory for the selected micromechanical sensor. With the implementation of mathematical substitutions, we developed a model for a system with distributed mass and analysed the behaviour of the sensor with SPICE3 and HSPICE simulator.

A comparison of the results acquired by the simulation with HSPICE to those of the MATLAB shows, that an error introduced with mathematical substitutions is one order of magnitude smaller than the resolution of the sensor.

The described model allows us to predict the behavior of the micromechanical part, and to simulate close loop measurements.

References

/1/ L.Hermans: "Trends in Microsystems", IMEC, ARRM 1996

/2/ Ljubisa Ristic (editor): "Sensor Technology and Devices", Artech House, 1994

/3/ E. P. Popov: "Engineering Mechanics of Solids", rentice Hall, New Jersey, 1990

/4/ Marko Škerlj: "Mehanika - trdnost", Fakulteta za strojništvo, Ljubljana, 1971

/5/ Francis Westo Sears: "Electricity and Magnetism", Addison-Wesley publ., 1958

/6/ K. Hackl, Technnische Univ. Graz, 1995, unpublished

/7/ J. Diaci, Fakulteta za strojništvo, 1995, unpublished

/8/ S. Marco, J. Samitier, O. Ruiz, A. Herms, J.R. Morante: "Analysis of electrostatic-damped piezoresistive silicon accelerometer", Sensors and Actuators, A, 37-38, pp. 317-322, 1993

/9/ J. Dominicus, I. Jntema, H.A.C. Tilmans: "Static and dynamic aspects of an air-gap capacitor", Sensors and Actuators, A35, 1992, pp. 121-128

/10/ D.E. Bergfried, B. Mattes, R. Rutz: "Electronic Crash Sensors for Restraint Systems", Proc. Int. Cong. on Transportation Electronics, Detroit, 1990, pp. 169-177

/11/ D.B. Herbert: "Simulating Differential Equations with SPICE2", Simulation and Modeling, Editor: Ping Yang, Circuit & Devices, Jan. 1992, pp. 11-14

/12/ G. Pelz, J. Bielefeld, F.J. Zappe, G. Zimmer: "Simulating Micro-Electromechanical Systems", Circuits & Devices, March 1995, pp. 10-13

/13/ G. Pelz, J. Bielefeld, G. Zimmer: "Model Transformation for Coupled Electro-mechanical Simulation in an Electronics Simulator"

/14/ G. Pelz, J. Bielefeld, F.J. Zappe: "MEXEL - Model-Conversion: Mechanics to Electronics", April 1995

/15/ R.M. Gutkowski: "Structures, Fundamental Theory and Behaviour", Van Nostrand Reinhold Co., New York, 1981

doc.dr. Janez Diaci, dipl. ing.
Faculty of Mechanical Engineering
Aškerčeva 25, 1000 Ljubljana, Slovenia
Tel.: +386 61 1771 429,
Fax. : +386 61 218 567
e-mail: janez.diaci@fs.uni-lj.si

prof.dr. Lojze Trontelj, dipl. ing.
dr. Vinko Kunc, dipl. ing.
e-mail: vinko@lm.eunet.si
dr. Igor Zelinka, dipl. ing.
e-mail: zigor@lm.eunet.si
Faculty of Electrical Engineering
Tržaška 25, 1000 Ljubljana, Slovenia
Tel.: +386 61 1768 337
Fax. : +386 61 126 46 44

Prispelo (Arrived): 06.02.1997 Sprejeto (Accepted): 25.02.1997